12 Particle physics with the CMS experiment at CERN

E. Aguiló, C. Amsler, V. Chiochia, S. de Visscher, C. Favaro, M. Ivova Rikova, B. Millán Mejías, P. Robmann, H. Snoek, S. Taroni, S. Tupputi, and M. Verzetti

in collaboration with the:

(CMS - Collaboration)

The Compact Muon Solenoid (CMS) experiment at the Large Hadron Collider (LHC) participates in one of the most challenging scientific endeavours, the search for the Higgs boson and other elementary particles. In 2012 the CMS experiment has significantly increased the size of the collected datasets, reaching a delivered integrated luminosity of 23.3 fb^{-1} at the center-of-mass energy $\sqrt{s} =$ 8 TeV, as shown in Fig. 12.1. The samples delivered in 2011 and 2010 at $\sqrt{s} = 7$ TeV correspond to an integrated luminosity of 6.1 fb^{-1} and 44.2 pb^{-1}, respectively. The LHC concluded the first three-year running period on February 14, 2013 and entered a two-year shutdown period (Long Shutdown 1, LS1). Proton beams colliding at the center-of-mass energy of 13 TeV are expected in early 2015.

2012 was a very productive year for CMS, with over hundred articles published in refereed journals. The year constitutes a real milestone for particle physics with the discovery of a Higgs-like boson in July by ATLAS and CMS. In this period, several members of our group played important coordination roles within the collaboration. One of us (V. C.) co-chaired the B-physics analysis group, that has so far released eighteen journal articles on quarkonium, b hadron decays and b-quark production measurements. H. S. convened the pixel calibration and reconstruction group and S. d.V. coordinated the simulation efforts in the standard model (SM) physics group.

In this report we describe the recent contributions of our group to the CMS experiment in the field of Higgs boson searches, measurements of SM processes and heavy flavour physics. In early 2012 we observed a new *usb*-baryon (the first new particle observed by CMS before the Higgs discovery) decaying into $\Xi_b^- \pi^+$, followed by $\Xi_b^- \to J/\psi\, \Xi^-$, with $J/\psi \to \mu^+\mu^-$ and $\Xi^- \to \Lambda\pi^-$, $\Lambda \to \pi^- p$. We observed 29 candidates (with a background of 6.6 $\pm$ 2.6) and obtained a mass of 5944.9 $\pm$ 2.8 MeV. This state is 154 MeV heavier than the spin 1/2 Ξ_b^-. According to theoretical models this would be the Ξ_b^{*0} with spin $\frac{3}{2}$. Details can be found in a recent CMS publication [1] and in our previous (2011) annual report. Furthermore, we discuss the performance studies done on the pixel detector, the innermost component of the CMS experiment. This detector was developed and commissioned by our group in col-

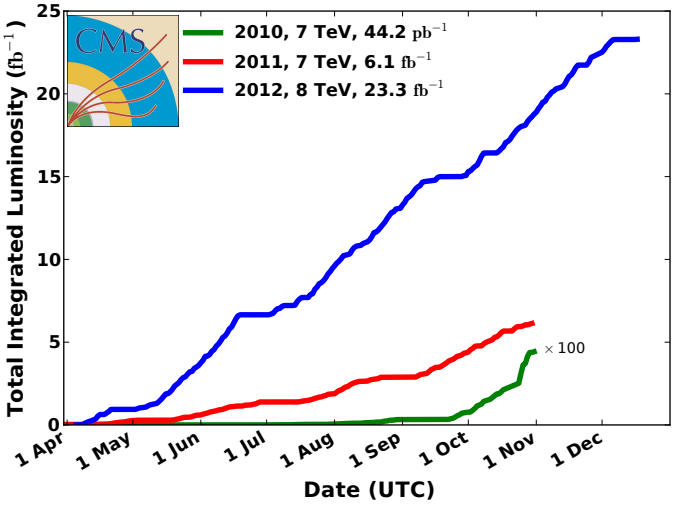

FIG. 12.1 – Cumulative luminosity delivered to CMS for p-p collisions during the three years of operation.

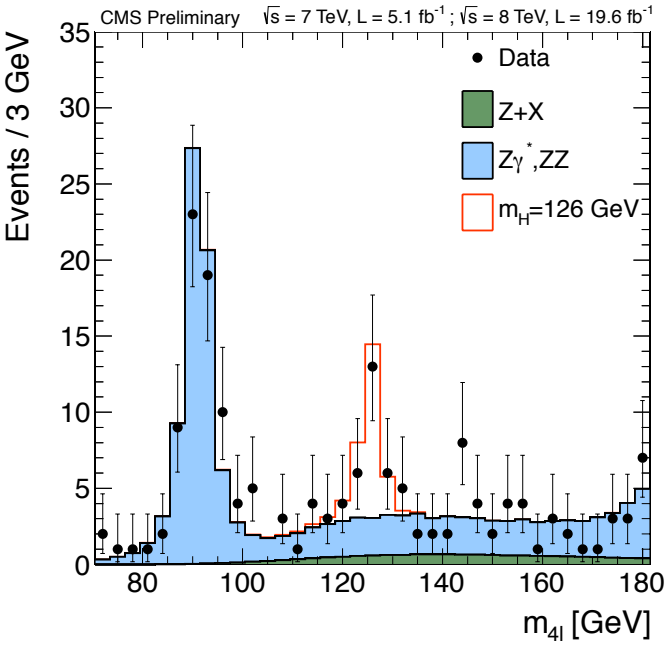

FIG. 12.2 – Distribution of the four-lepton reconstructed mass for the sum of the $4e$, 4μ, and $2e+2\mu$ channels. Measured data are compared with predictions for background and the signal for a Higgs boson at 126 GeV.

laboration with PSI and ETH Zurich. It allows the precise reconstruction of charged particle tracks as well as the identification the primary collision vertex and secondary vertices from long-lived particles. This device is crucial for our research using b-quarks and tau-leptons.

[1] CMS Collaboration, Phys. Rev. Lett. **108** (2012) 252002.

12.1 Higgs boson searches in tau pairs

On July 4, 2012 the CMS and ATLAS collaborations announced the observation of a Higgs-like resonance with a mass of about 126 GeV [1, 2]. The resonance was observed with significance larger than three standard deviations in decays to pairs of vector bosons, such as W^+W^-, ZZ, and $\gamma\gamma$. The analysis of all the data collected until the end of 2012 further consolidated the evidence for a new particle. Figure 12.2 shows the invariant mass distribution of ZZ candidates with decaying into four leptons from the combined analysis of the complete 2011 and 2012 datasets [3]. A clear excess is observed slightly above 120 GeV with a local significance of about 7 standard deviations. The mass determined from a combination of the three leptonic channels ($4e$, 4μ, $2e+2\mu$) is $125.8 \pm 0.4(\text{stat.}) \pm 0.2(\text{syst.})$ GeV. The signal strength modifiers associated with the vector bosons and fermions in production were found to be consistent with the SM expectations. The spin-parity of the boson was also studied and the pure scalar hypothesis ($J^P = 0^+$) was found to be consistent with the observation when compared to six other spin-parity hypotheses [3, 4].

In the fermionic decay channels, such as $\tau^+\tau^-$ and $b\bar{b}$, the observed excess with respect to background expectation is below three standard deviations. Of particular interest is the decay mode into two tau leptons, which is expected to have the second largest branching ratio for a mass of 126 GeV, with relatively small background. Among the possible production modes and final states our group focused on the associate production of a Higgs boson and a Z or W boson [5]. While this production mode has a lower cross section than the direct production, it has a smaller background and may allow a better measurement of the Higgs coupling constant with the tau leptons in the future.

Three- and four-lepton events were used to search for Higgs bosons produced in association with vector bosons, with the leptonic decay of the W boson (WH) or Z boson (ZH), respectively. The search for WH production was performed in three-lepton final states. Two final states with two light leptons and a hadronic tau decay, $e\mu\tau_h$ and $\mu\mu\tau_h$, and two final states with one lepton and two hadronic tau decays, $e\tau_h\tau_h$ and $\mu\tau_h\tau_h$, were considered. The resulting invariant mass distribution of the event candidates with two light leptons and a hadronic tau decay is shown in Fig. 12.3. The search for ZH production was performed in four-lepton events

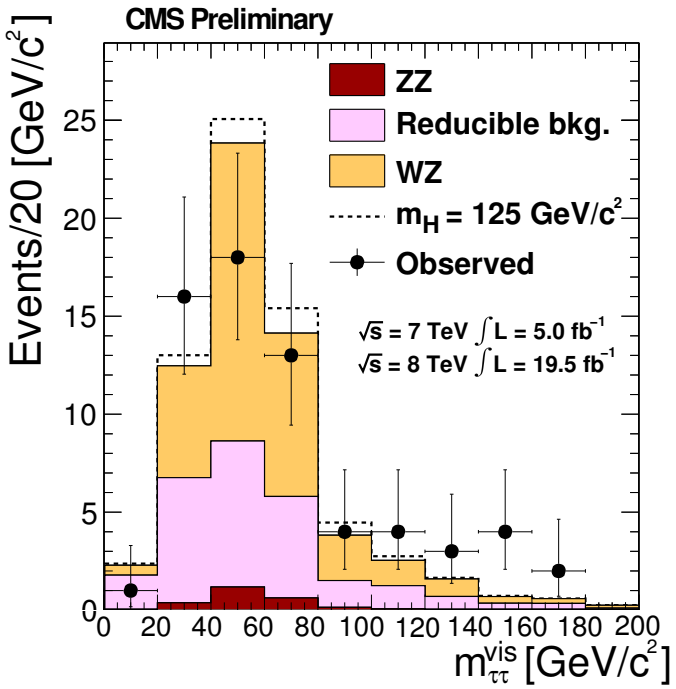

FIG. 12.3 – Observed and expected Higgs boson candidate mass spectra in the channels with two leptons and a hadronic tau decay. The expected contribution from the associated production of a SM Higgs boson with mass of 125 GeV is shown by the dashed line.

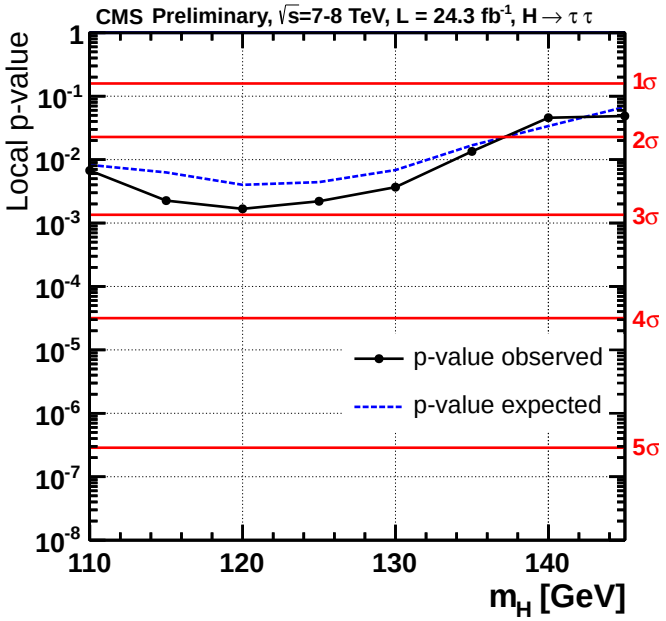

FIG. 12.4 – Observed and expected p-value $1 - \text{CL}_b$, and the corresponding significance in number of standard deviations for the combination of Higgs boson searches in tau pairs.

with a pair of electrons or muons consistent with the decay of a Z boson, and a Higgs boson candidate with one of the following final states: $e\mu$, $e\tau_h$, $\mu\tau_h$, or $\tau_h\tau_h$. In all channels the data were found to be compatible with both the background-only prediction and the presence of a SM Higgs boson.

The results of this analysis were combined with the inclusive Higgs boson search in tau decays. In this analysis the tau-lepton pair invariant-mass spectrum was studied in five different final states corresponding to the decay modes of the two tau leptons. After the combination an excess of events was observed over a broad mass range, with a maximum local significance of 2.9 standard deviations at a mass of 120 GeV, as shown in Fig. 12.4. This excess is compatible with the presence of a SM Higgs boson of mass 125.8 GeV, for which the local significance is 2.85 σ. This is an indication that the new boson discovered on July 4, 2012 couples to τ leptons, with a strength compatible to the one predicted by the SM.

Our group also had a strong involvement in the validation and data quality monitoring (DQM) of tau lepton identification in CMS. The DQM system provides basic information on the collected data once the events are reconstructed. This information is used to establish whether a given period of data taking is suitable for further analysis or not, and to check the functionality of the event reconstruction algorithms. In 2012 our group has implemented the necessary DQM software for the tau identification and further improved it following the feedback collected during data taking operations.

[1] S. Chatrchyan *et al.* [CMS Collaboration], Phys. Lett. B **716** (2012) 30.

[2] G. Aad *et al.* [ATLAS Collaboration], Phys. Lett. B **716** (2012) 1.

[3] S. Chatrchyan *et al.* [CMS Collaboration], CMS-PAS-HIG-13-002.

[4] S. Chatrchyan *et al.* [CMS Collaboration], Phys. Rev. Lett. **110** (2013) 081803.

[5] S. Chatrchyan *et al.* [CMS Collaboration], CMS-PAS-HIG-12-053.

12.2 Angular correlations of b hadrons in association with a Z boson

The production of b-quark pairs in association with Z bosons is the main SM background to the Higgs boson searches in b-quark decays and other searches for new physics. Monte Carlo (MC) simulations of this process have been performed assuming massive or massless b quarks, usually referred as four- and five-flavor calculation schemes, respectively. The validation of the different calculation techniques is of great importance for the correct background estimates in future searches.

Our group performed the measurement of the total cross section and angular correlations of b hadrons produced in this process, using a data sample corresponding to an integrated luminosity of 5 fb^{-1} at the center-of-mass energy of 7 TeV [1, 2]. Four variables were considered to describe the angular correlations of the final-state particles:

- the three-dimensional and transverse angular separation between the b hadrons (ΔR_{BB} and $\Delta\phi_{BB}$), sensitive to the $pp \to Z + b\bar{b}$ production mechanism,

- the three-dimensional angle between the Z boson momentum and the closest B hadron ($\min\Delta R_{ZB}$), and

- the asymmetry between the Z boson momentum and the b-hadron system, which are affected by the additional parton radiation.

The cross sections are evaluated in several regions of the Z boson transverse momentum, p_T. The total cross section as a function of the Z p_T was also measured.

Events containing a Z boson decay were selected by requiring the presence of two isolated leptons — muons or electrons — with opposite charge, high p_T, and invariant mass in the Z boson mass range. B hadrons were identified through the displaced vertices from their decays, using the inclusive vertex finder (IVF) technique. The IVF algorithm is independent from jet reconstruction, hence it does not suffer from the geometrical limitations due to the jet cone size and can access collinear b hadron production. Only events with two reconstructed B hadron candidates with $p_T > 8$ GeV and pseudorapidity $|\eta| < 2.0$ were retained. Additional requirements were imposed on the decay vertex invariant mass and decay length to reduce the contamination from charm quark decays.

The differential cross section as a function of ΔR_{BB} and the total cross section for different requirements on the Z boson p_T are shown in Fig. 12.5 and Fig. 12.6, respectively. The measurements are compared to the tree-level predictions by MADGRAPH MC, in the four- and five-flavour calculation schemes. The four-flavour predictions provide the best description of the measured data.

In parallel with the data analysis we have also worked on improving the simulation of this process with MADGRAPH 5. In particular, we have optimised the four-flavour jet matching technique, which is relevant for processes with one or more massive quarks emitted from the initial or final state radiation, such as $Z + b\bar{b}$, $W + b\bar{b}$, $t(W)/b$, and $H + b\bar{b}$. The new MAD GRAPH release is expected to be an important improvement for future searches.

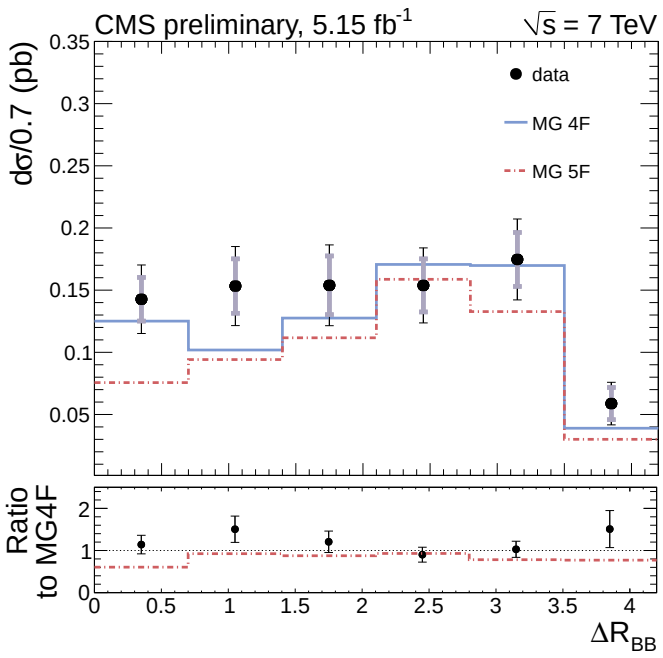

FIG. 12.5 – Differential cross section for pp → Zbb̄ as a function of the three-dimensional angle between the b hadrons, ΔR_{BB}. Measured data are compared with MADGRAPH MC predictions for the four- and five-flavor schemes.

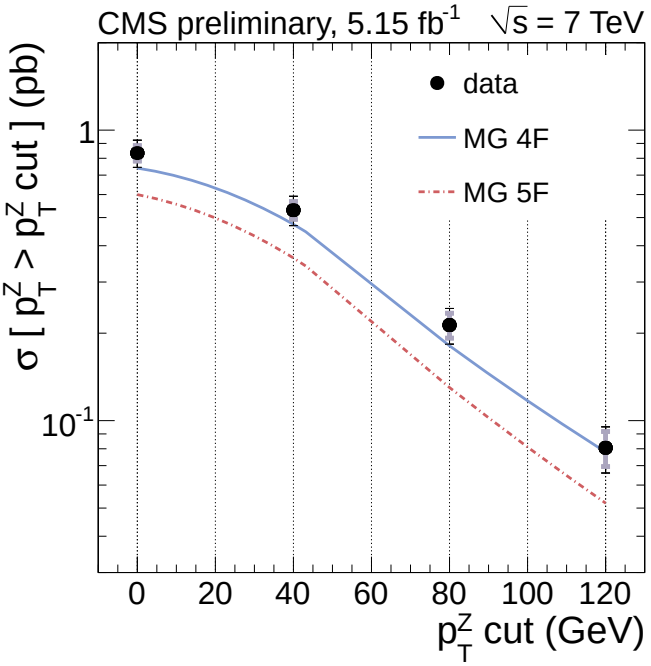

FIG. 12.6 – Total pp → Zbb̄ production cross section as a function of the minimum Z boson p_T.

[1] S. Chatrchyan *et al.* [CMS Collaboration], CMS-PAS-EWK-11-015.

[2] C. Favaro, PhD-thesis, Universität Zürich (in preparation)

12.3 Polarization of the Λ_b baryon

Polarization studies in b baryon decays provide important information on heavy quark decay dynamics [1]. We performed a measurement of the Λ_b polarization in pp collisions at 7 TeV using the decay sequence $\Lambda_b \to J/\psi(\to \mu^+\mu^-)\Lambda(\to p\pi^-)$ [2]. From a sample of 5 fb^{-1} of integrated luminosity we obtained ∼1800 reconstructed Λ_b and $\overline{\Lambda}_b$ candidates (the $\overline{\Lambda}_b$ decaying into the charge conjugated particles). The $(J/\psi)\Lambda$ invariant mass distribution shows a pronounced peak on top of a ∼ 10% continuous background.

The analysis exploits the angular correlations between the daughter particles. The physics parameters (such as polarization and analyzing power) are extracted by a multi-dimensional likelihood fit to the angular distributions. Three angular distributions are employed: $\cos\theta_\Lambda$, $\cos\theta_p$ and $\cos\theta_\mu$, where θ_Λ, θ_p and θ_μ are the polar angles of the Λ, the proton and the μ^+ in the rest frames of Λ_b, Λ and J/ψ, respectively, as shown in Fig. 12.7. The distortions of the angular distributions caused by the geometrical acceptance of the detector and the event selection are determined by Monte Carlo simulation. The contribution from background is determined with data events in the sidebands of the Λ_b mass peak. For a better separation of signal and background the mass distribution is also included in the fit. Note that the polarizations of the Λ_b and $\overline{\Lambda}_b$ are not necessarily equal since their production mechanisms are not identical. Each step of the analysis is therefore performed independently for Λ_b and $\overline{\Lambda}_b$.

Figure 12.8 shows the measured angular and mass distributions together with the fits for Λ_b candidates. Similar fits are also performed for the antiparticles. The fit is performed on events within the mass peaks. Our preliminary results show that both Λ_b and $\overline{\Lambda}_b$ are produced with polarizations smaller than 10%. We find for the polarizations of the Λ_b and $\overline{\Lambda}_b$, $P_{\Lambda_b} = 0.03 \pm 0.09 \pm 0.02$ and $P_{\overline{\Lambda}_b} = 0.02 \pm 0.08 \pm 0.05$, respectively, where

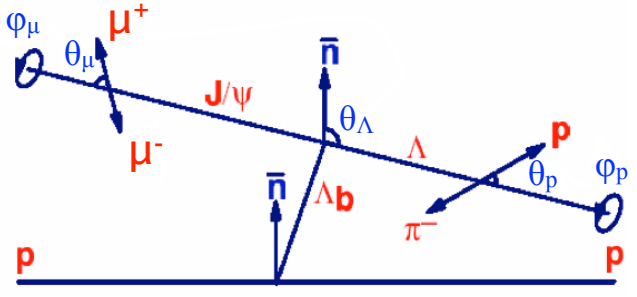

FIG. 12.7 – Definitions of the reference frames and angles used in the Λ_b polarization analysis.

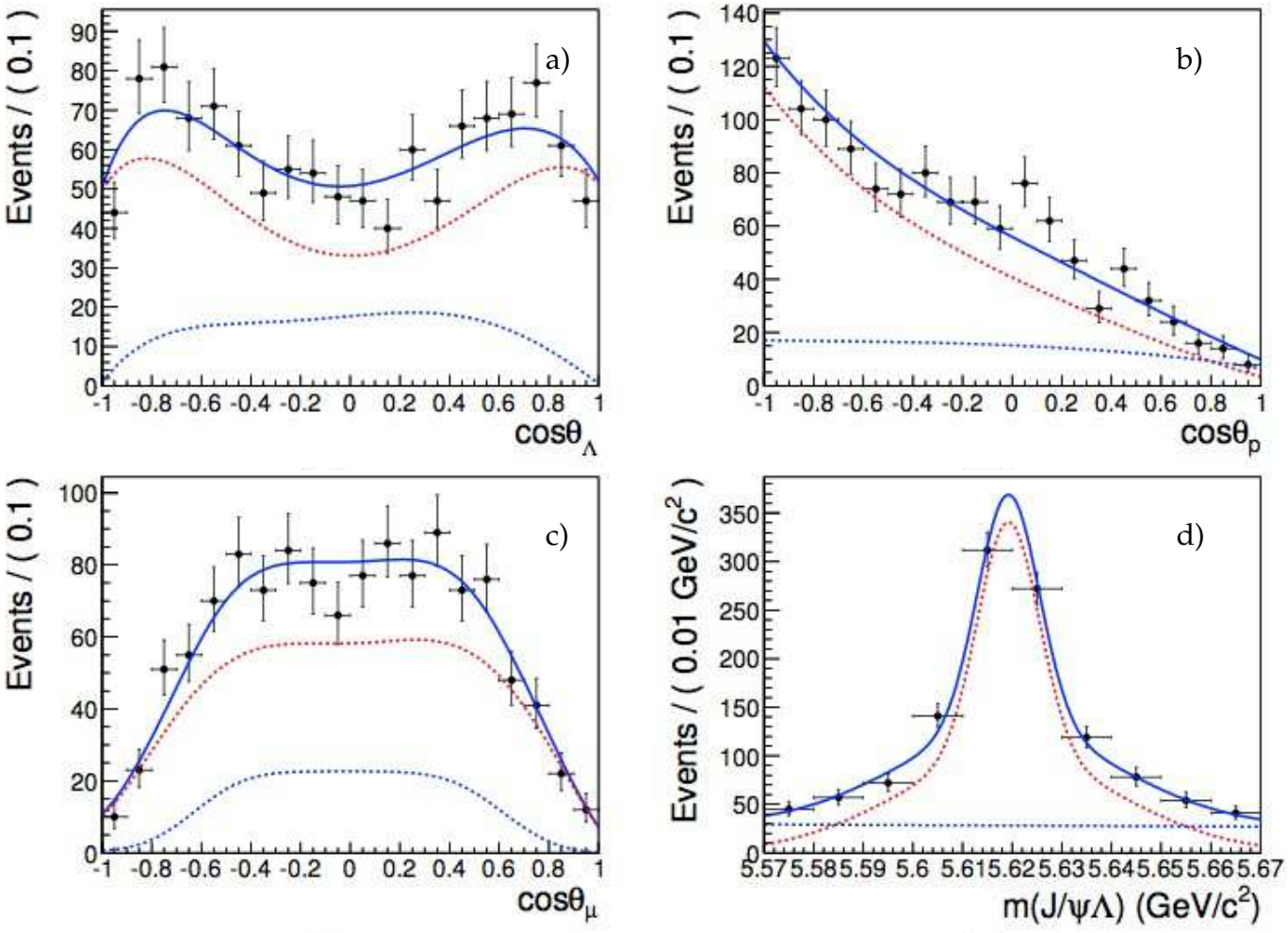

FIG. 12.8 –
a) Angular distribution of the Λ in the Λ_b rest frame; b) angular distribution of the proton in the Λ rest frame; c) angular distribution of the muon in the J/ψ rest frame; d) mass distribution in the Λ_b region. The black dots represent the measured data. The lines show the results from a multi-dimensional likelihood fit: total fit (solid blue), signal folded with efficiency (dashed red) and background contribution (dashed blue).

the first uncertainty is statistical and the second systematic. These results are compatible with expectations from perturbative QCD which predict polarization not exceeding 10% in high energy pp collisions [3]. Our results agree with a recent measurement from LHCb which, however, does not distinguish between Λ_b and $\overline{\Lambda}_b$ [4].

[1] M. Krämer and H. Simma, Nucl. Phys. **B 50** (1996) 125

[2] M. Ivova Rikova, PhD-thesis, Universität Zürich (Submission in June 2013)

[3] G. Hiller *et al.*, Phys. Lett. **B 649** (2007) 15

[4] LHCb Collaboration, arXiv:1302.5578 (2013)

12.4 Lifetime of the B_s meson

Our analysis focuses on the study of the B_s meson decaying into $(J/\psi)\phi$, where J/ψ decays into two muons of opposite charges, and $\phi(1020)$ into two kaons of opposite charges ($B_s \to J/\psi\,[\to \mu^+\mu^-]\,\phi[\to K^+K^-]$) [1]. We are measuring the width difference $\Delta\Gamma_s = \Gamma_L - \Gamma_H$ of the two CP-eigenstates of the B_s-meson, B_L (CP $= +1$) and B_H (CP $= -1$). $\Delta\Gamma_s$ is positive [2] and the CP-violating phase ϕ_s is set to zero. This phase has been measured [3], $\phi_s = 0.07 \pm 0.09$, and is indeed predicted to be small in the SM, $\phi_s = -0.036 \pm 0.002$.

Since the B_s meson is pseudoscalar and the J/ψ and $\phi(1020)$ are vectors, the orbital angular momentum of the two decay products is $L = 0$, 1, or 2. For L even we have thus CP $= +1$ (B_L), for L odd CP $= -1$ (B_H). Hence the angular correlations between the decay products are different for the two states [4, 5].

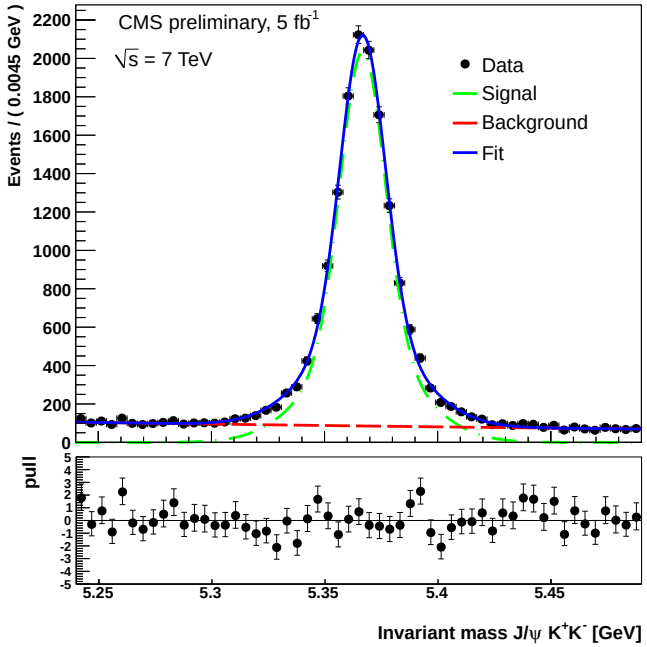

FIG. 12.9 – Invariant mass distribution of the B_s candidates (see legend).

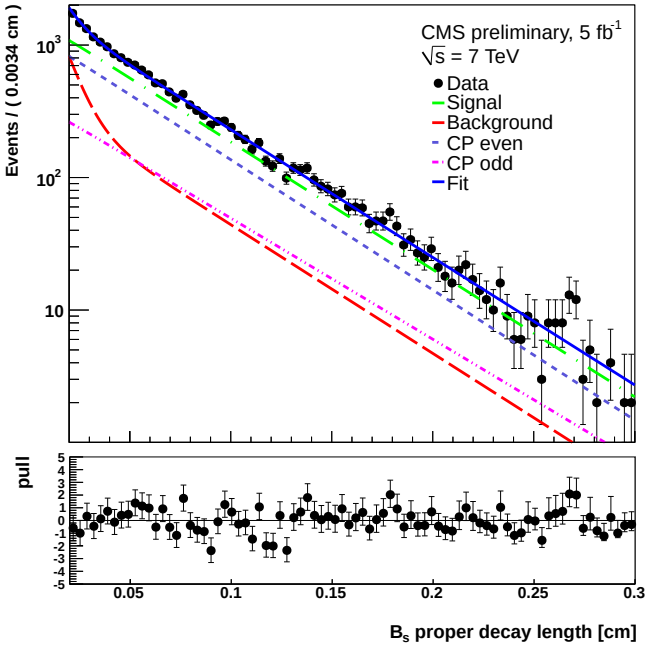

FIG. 12.10 – Projection of the proper decay length from the 5D maximum likelihood fit (see legend).

The following cuts are applied to select the $B_s \to (J/\psi)\phi$ candidates:

- Two muons emerge from a secondary vertex as expected from a J/ψ decay.
- Their invariant mass is equal to the J/ψ mass within $\pm 150\ \mathrm{MeV/c^2}$.
- Their transverse momentum is larger than 7 GeV/c.
- The transverse momentum of the kaon pair is larger than 0.7 GeV/c.
- Their invariant mass is equal to the $\phi(1020)$ mass within $\pm 5\ \mathrm{MeV/c^2}$.

The selected events show a pronounced peak of 19 200 B_s events in the B_s invariant mass distribution, as shown in Fig 12.9.

The likelihood analysis is based on probability density functions (PDF) for signal and background. The signal PDF is from a theoretical model that includes the fit parameters [4, 5]. The background PDF is parameterized with an empirical model. A one-dimensional mass fit is performed first on the B_s candidates between 5.24 and 5.49 GeV. The sidebands are then fitted with the empirical model. In the final step the full likelihood fit is performed.

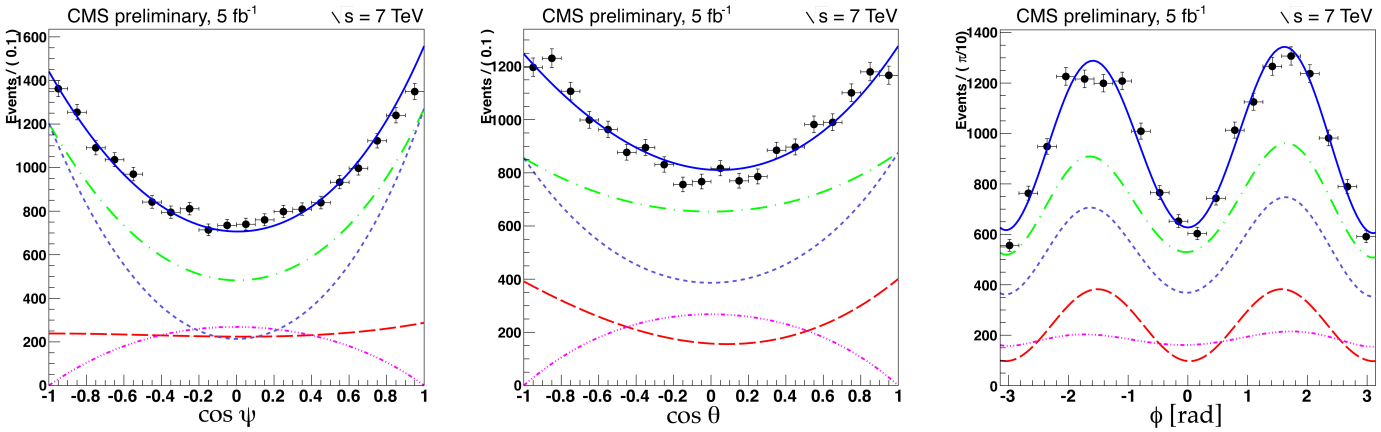

FIG. 12.11 – Angular distributions of $\cos\psi$, $\cos\theta$ and ϕ (see text). The solid blue lines are the fit, the green lines the signal component, the red lines the background component, and the black points are the data. The magenta dashed line are the CP odd component, the purple dashed line the CP even component.

TAB. 12.1 –
Measurements of Γ_s and $\Delta\Gamma_s$ from $B_s \to (J/\psi)\phi$ at the LHC. The SM prediction is $\Delta\Gamma_s = 0.147(60) \times \Gamma_s = 0.097(39)\ ps^{-1}$.

Experiment	Γ_s [ps^{-1}]	$\Delta\Gamma_s$ [ps^{-1}]
CMS [6]	0.655(10)	0.048(24)
ATLAS [7]	0.677(8)	0.053(23)
LHCb [3]	0.663(8)	0.100(17)

Figure 12.9 and 12.10 show the fits on the invariant mass and the lifetime distributions, respectively. Figure 12.11 shows the angular distributions. The angles θ and ϕ denote the flight direction (polar and azimuthal angles) of the μ^+ in the J/ψ rest frame. The angle ψ is the polar angle of the K^+ in the rest frame of the $\phi(1020)$ with respect to the negative B_s flight direction [1]. From the 19 200 candidates we find $14\,310 \pm 138$ B_s events, leading to a mean mass of $5\,366.8 \pm 0.1$ MeV [6]. We also obtain $\Delta\Gamma_s = 0.048 \pm 0.024\ (stat.) \pm 0.003\ (syst.)\ ps^{-1}$, and $\tau_{B_s} = 1.528 \pm 0.020\ (stat.) \pm 0.010\ (syst.)$ ps. Our measurements are compared with the ATLAS and LHCb results in Table 12.1, where the systematic and statistical uncertainties are added in quadrature. The LHC results are in good agreement with predictions from the SM.

[1] B. Millán Mejías, PhD-thesis, Universität Zürich (Submission in June 2013)

[2] LHCb Collaboration, Phys. Rev. Lett. **108** (2012) 241801

[3] LHCb Collaboration, arXiv:1304.2600 (2013)

[4] A.S. Dighe, I. Dunietz and R. Fleischer, Eur. Phys. J. **C 6** (1999) 647

[5] I. Dunietz, R. Fleischer and U. Nierste, Phys. Rev. **D63** (2001) 114015

[6] S. Chatrchyan *et al.* [CMS Collaboration], CMS PAS BPH-11-006.

[7] ATLAS Collaboration, arXiv: 1208.0572 (2013)

12.5 Studies of pixel detector performance and improvements to the hit reconstruction

The CMS pixel detector is the innermost tracking device of the CMS experiment, providing charged particle trajectories and production vertices. It includes three cylindrical layers in the barrel region and four end cap disks, two at each side of the barrel. The three layers are located at 4.4, 7.3, and 10.2 cm from the beam axis. Due to the short distance to the interaction region the detector operates in a very harsh environment characterised by a high radiation dose. The current pixel detector must operate until the second LHC long shutdown, foreseen in 2017. A detailed study of its current performance and the comparison with the detector simulations are required for the optimal continuation of the physics program.

The pixel detector plays a key role in the reconstruction of charged particles in CMS. A particle passing through the silicon sensors deposes charge and activates "clusters" of consecutive pixels above the readout threshold. The cluster shape and the deposited charge is used by the reconstruction algorithms to determine the track incident point and its uncertainties. Since the hit detection efficiency was found to be dependent on the instantaneous luminosity, our group has studied the dependence of the cluster size and charge. The instantaneous luminosity was about $7 \times 10^{33}\ cm^{-2}s^{-1}$ at the beginning of a data taking run and decreased of a factor 3 before beams were dumped and new beams were injected in the accelerator. To simulate the varying conditions, we divided the analysed run into 20 subsamples corresponding to different instantaneous luminosities and for each subsample we have simulated a dedicated MC sample using the corresponding distribution of simultaneous collisions extracted from measured data. While no significant dependence of the cluster size was observed on the instantaneous luminosity, the collected charge shows interesting features.

The average cluster charge increases with the distance from the interaction point as expected from the decreasing irradiation dose. The difference in collected charge between layers can be as large as 11%. Furthermore, we observed a dependence of the cluster charge on the instantaneous luminosity. The most probable value (MPV) of the cluster charge distribution was measured as function of the instantaneous luminosity fitting the data with a Landau convoluted with a Gaussian, as shown in Fig. 12.12. The effect is most prominent in the innermost layer, where the MPV was found to decrease by about 6% within a data taking run. The effect is currently attributed to the operating temperature of the pixel readout electronics, which is expected to be higher at larger particle occupancies. Further studies of the charge collection are currently in progress.

When two charged particles traverse the sensitive material in close proximity, the clusters overlap and merge into one larger cluster. In the innermost layer of the pixel detector this effect occurs if the opening angle between the two particle trajectories is below 5 mrad. For a typical three-prong τ decay this corresponds to a transverse momentum of about 150 GeV. The merging of clusters deteriorates the measurement of the particle trajectories through the tracking volume and the reconstruction of the τ lepton and of the b-quark jets.

We have shown that merged clusters can be identified by calculating the charge deposited in the cluster corrected for the incident angle of the trajectory. The incident angle is determined assuming a straight line from

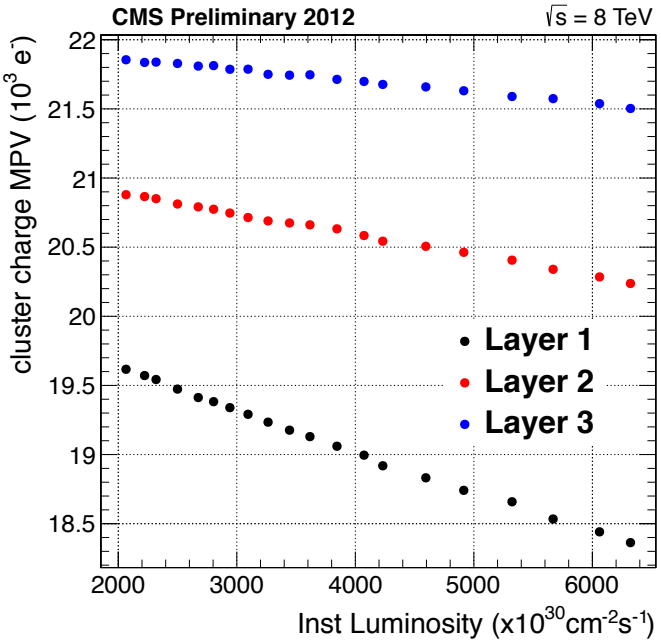

FIG. 12.12 –
Most probable value of the pixel cluster charge as function of the instantaneous luminosity. The datasets correspond to the three layers of the barrel pixel detector.

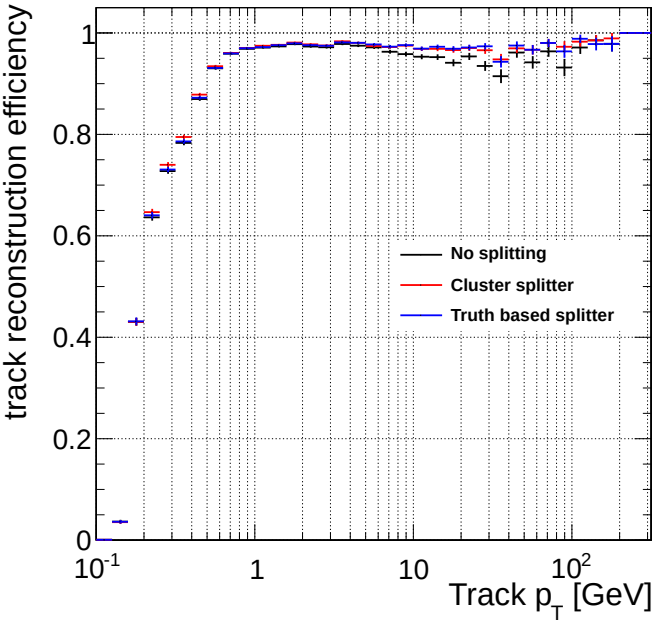

FIG. 12.13 –
Track reconstruction efficiency for boosted top events with and without the pixel hit splitting technique.

the vertex in the event with the highest summed transverse momentum. This hypothesis works well for the high momentum tracks that are usually associated to the origin of merged clusters. Two template clusters are fit to the identified merged cluster and replace the merged cluster for the subsequent tracking algorithms.

We have recently tested the algorithm both on simulated collision events and on data. Figure 12.13 shows the track reconstruction efficiency in a sample of boosted top quark pairs. The default tracking algorithm (black) is compared to the ideal scenario without cluster merging (red) and to the cluster splitting algorithm (blue). Clear improvement is observed for the high transverse-momentum tracks. For tracks with $p_T > 10$ GeV the efficiency enhancement can be up to 5%. We are currently finalising the implementation of the new algorithm in the CMS reconstruction software and we plan to utilise it in several physics analyses.